ISSN 1392–1207. MECHANIKA. 2017 Volume 23(5): 678–687

Free Vibrational Response of Single-Layered Graphene Sheets Embedded in an Elastic Matrix using Different Nonlocal Plate Models

Babak SAFAEI, A.M. FATTAHI*
**Department of Mechanical Engineering, Tabriz Branch, Islamic Azad University, Tabriz, Iran,*
E-mail: a.fattahi@iaut.ac.ir

crossref http://dx.doi.org/10.5755/j01.mech.23.5.14883

1. Introduction

Owing to their outstanding mechanical, electrical, and chemical properties, the family of carbon allotropes including carbon nanotubes, graphene sheets and fullerenes are becoming increasingly important in the emerging field of nanoscience and nanotechnology [1-2]. Technical difficulties in conducting experiments at the nanoscale make it necessary to have recourse to theoretical approaches for investigating the behaviour of nanostructures.

Based on the classical plate theory (CLPT), Kitipornchai et al. [3] investigated the vibration response of multi-layered graphene sheets (MLGSs) with simply-supported boundary conditions using a continuum model. They proposed an explicit formula for the van der Waals interaction between any two sheets in a MLSG. Liew and his coworkers [4] proposed a continuum model to analyse the vibrations of MLSG embedded in an elastic matrix.

Because of not having the capability of considering the size-effects, the implementation the classical continuum models to predict the behaviour of nanostructures becomes controversial. Hence, the extension of the continuum mechanics to accommodate the size dependence of nanostructures is a topic of major concern. Modified continuum models are one of the most applied theoretical approaches for the investigation of nanomechanics due to their computational efficiency and the capability to produce accurate results which are comparable to those of atomistic models. The application of nonlocal continuum mechanics allowing for the small scale effects to the vibrational analysis of nanomaterials has been recommended by many research workers.

Azizi et al. [5-6] using carbon nanotubes as reinforcing fibres have been performed to address the exceptional mechanical and electrical properties of nanotube-based composites. Vibration analysis of MLGSs embedded in polymer matrix was investigated by Pradhan and Phadikar [7] using nonlocal continuum mechanics.

Continuing with the vibration problems, Pradhan et al. [8] developed a single-elastic beam model to analyse the thermal vibration of CNTs based on thermal elasticity mechanics, and nonlocal elasticity theory. The effect of nonlocal scale parameter on the wave propagation in multi-walled carbon nanotubes was represented by Narendar and Gopalakrishnan [9]. Murmu and Pradhan [10] studied the vibration characteristics of single-walled carbon nanotubes (SWCNTs) based upon a nonlocal shell model.

There are so many other researches in which the behaviours of nanostructures under various loading conditions have been predicted based on nonlocal elasticity continuum models [11-20] which indicate the wide application of this type of modified continuum mechanics in nanomechanics.

In many cases such as polymer nanocomposites, the nanostructures can be embedded in an elastic surrounding medium. This elastic medium is generally simulated using Winkler foundation model [21]. Based on this type of foundation, the elastic matrix is represented as a series of closely spaced, vertical linear elastic springs. However, this model does not have the capability to consider the continuity of the medium. A more practical modelling of elastic foundation can be implemented using Pasternak foundation model [22] which regards both normal pressure and transverse shear stress using two modulus parameters corresponding to each one. The Pasternak foundation model was used by Pradhan and Murmu [23], and Liew et al. [24] to simulate the interaction of the elastic medium with graphene sheet and successful results were obtained to show the physically realistic application of this type of foundation modelling.

According to the above literature review, it can be seen that the investigation of size-effects on behaviours of nanostructures has assigned so many researches. In the current study, the free vibrational response of SLGSs embedded in an elastic medium is investigated based on various nonlocal plate models. Both Winkler and Pasternak elastic foundation models are employed to represent the surrounding elastic matrix. Closed-form analytical solution is developed to obtain explicit formulas to obtain the natural frequencies of SLGSs corresponding to each type of nonlocal plate theory through exact solution for the governing differential equations. Selected numerical results are presented to show the influence of nonlocality, elastic foundation, type of nonlocal plate theory and side length of square SLGSs in detail.

2. Overview of various plate theories

2.1. Introduction

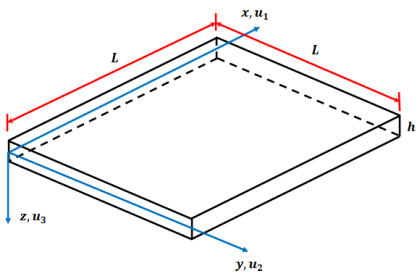

Fig. 1 Schematic of a nanoplate: kinematic parameters, coordinate system and geometry

To represent the behaviour of plates, there are different plate theories. As it can be seen from Fig. 1, consider a uniform square nanoplate with the side length *L* and thickness *h*. A coordinate system (*x*, *y*, *z*) is introduced at the one corner of the midplane of the nanoplate, whereas the *x* axis is taken along the length of the nanoplate, the y axis in the width direction and the z axis is taken along the depth (thickness) direction. The displacement components (u_1, u_2, u_3) along the axes (*x*, *y*, *z*) can be written in a general form as:

$$u_1 = -z\frac{\partial w}{\partial x} + \psi(z)\left(\frac{\partial w}{\partial x} + \varphi_x\right), \tag{1-a}$$

$$u_2 = -z\frac{\partial w}{\partial y} + \psi(z)\left(\frac{\partial w}{\partial y} + \varphi_y\right), \tag{1-b}$$

$$u_3 = w(x,t), \tag{1-c}$$

where w is the transverse displacement or displacement in z direction and φ_x ,φ_y are the angular displacements in the x and y directions, respectively. $\psi(z)$ is the shape function as follows: For classical plate theory (CLPT): $\psi(z) = 0$

For first order shear deformation theory (FSDT): $\psi(z) = z$ For higher order shear deformation theory (HSDT):

$$\psi(z) = z - \frac{4z^3}{3h^2}$$

2.2. Classical plate theory (CLPT)

The simplest and the most well-known plate theory is the classical plate theory in which it is assumed that the straight lines which are vertical to the mid-plane will remain straight and vertical to the mid-plane after deformation. In other words, the effects of shear deformation and rotational inertia are not considered in this type of plate theory. On the basis of Eq. (1), the strain-displacement relations appropriate to CLPT can be obtained as:

$$\varepsilon_{xx} = \frac{\partial u_1}{\partial x} = -z\frac{\partial^2 w}{\partial x^2}, \tag{2-a}$$

$$\varepsilon_{yy} = \frac{\partial u_2}{\partial y} = -z\frac{\partial^2 w}{\partial y^2}, \tag{2-b}$$

$$\gamma_{xy} = \frac{\partial u_1}{\partial y} + \frac{\partial u_2}{\partial x} = -2z\frac{\partial^2 w}{\partial x \partial y}, \tag{2-c}$$

$$\gamma_{xz} = \gamma_{yz} = 0. \tag{2-d}$$

Using the principle of virtual displacement, the equilibrium equation can be expressed for CLPT as:

$$\frac{\partial^2 M_{xx}}{\partial x^2} + \frac{\partial^2 M_{yy}}{\partial y^2} + 2\frac{\partial^2 M_{xy}}{\partial x \partial y} = \rho h \frac{\partial^2 w}{\partial t^2}, \tag{3}$$

$$M = \left\{M_{xx}, M_{yy}, M_{xy}\right\}^T = \int_{-h/2}^{h/2} z\left\{\sigma_{xx}, \sigma_{yy}, \sigma_{xy}\right\}^T dz,$$

where *M* is torque, ρ is the mass density and σ is axial stress. The governing Eq. (3) can be obtained in terms of displacements as:

$$\frac{Eh^3}{12\left(1-\nu^2\right)}\left(\frac{\partial^4 w}{\partial x^4} + 2\nu\frac{\partial^4 w}{\partial x^2 \partial y^2} + \frac{\partial^4 w}{\partial y^4}\right) - \\ -\frac{Eh^3}{6\left(1+\nu\right)}\frac{\partial^4 w}{\partial x^2 \partial y^2} = \rho h \frac{\partial^2 w}{\partial t^2}, \tag{4}$$

where *E* and *v* are Elastic modulus and poison ration.

2.3. First order shear deformation theory (FSDT)

The next plate theory is the first order shear deformation theory in which the effects of shear deformation and rotational inertia are taken into account, so the straight lines will no longer remain vertical to the mid-plane of the plate after deformation. However, it is assumed that the transverse shear stress has a linear distribution along the thickness of the plate. Using Eq. (1), the following strain-displacement relations can be obtained as:

$$\varepsilon_{xx} = \frac{\partial u_1}{\partial x} = z\frac{\partial \varphi_x}{\partial x}, \tag{5-a}$$

$$\varepsilon_{yy} = \frac{\partial u_2}{\partial x} = z\frac{\partial \varphi_y}{\partial y}, \tag{5-b}$$

$$\gamma_{xy} = \frac{\partial u_1}{\partial y} + \frac{\partial u_2}{\partial x} = z\left(\frac{\partial \varphi_x}{\partial y} + \frac{\partial \varphi_y}{\partial x}\right), \tag{5-c}$$

$$\gamma_{xz} = \frac{\partial u_1}{\partial z} + \frac{\partial u_3}{\partial x} = \frac{\partial w}{\partial x} + \varphi_x, \tag{5-d}$$

$$\gamma_{yz} = \frac{\partial u_2}{\partial z} + \frac{\partial u_3}{\partial y} = \frac{\partial w}{\partial y} + \varphi_y. \tag{5-e}$$

Using the principle of virtual displacement, the equilibrium equations can be expressed for FSDT as:

$$\frac{\partial Q_{xx}}{\partial x} + \frac{\partial Q_{yy}}{\partial y} = \rho h \frac{\partial^2 w}{\partial t^2}, \tag{6-a}$$

$$\frac{\partial M_{xx}}{\partial x} + \frac{\partial M_{xy}}{\partial y} - Q_{xx} = \rho h^3 \frac{\partial^2 \varphi_x}{\partial t^2}, \tag{6-b}$$

$$\frac{\partial M_{yy}}{\partial y} + \frac{\partial M_{xy}}{\partial x} - Q_{yy} = \rho h^3 \frac{\partial^2 \varphi_y}{\partial t^2}, \tag{6-c}$$

where $Q = \left\{Q_{xx}, Q_{yy}\right\}^T = \int_{-h/2}^{h/2}\left\{\sigma_{xz}, \sigma_{yz}\right\}^T dz.$

The governing Eq. (6) can be obtained in terms of displacements as:

$$\kappa Gh\left(\frac{\partial\varphi_x}{\partial x}+\frac{\partial\varphi_y}{\partial y}+\frac{\partial^2 w}{\partial x^2}+\frac{\partial^2 w}{\partial y^2}\right)=\rho h\frac{\partial^2 w}{\partial t^2}, \quad (7\text{-a})$$

$$\frac{Eh^3}{12\left(1-\nu^2\right)}\left(\frac{\partial^2\varphi_x}{\partial x^2}+\nu\frac{\partial^2\varphi_y}{\partial x\partial y}\right)+\frac{Eh^3}{24\left(1+\nu\right)}\times$$
$$\times\left(\frac{\partial^2\varphi_x}{\partial x\partial y}+\frac{\partial^2\varphi_y}{\partial y^2}\right)-\kappa Gh\left(\varphi_x+\frac{\partial w}{\partial x}\right)=\rho h^3\frac{\partial^2\varphi_x}{\partial t^2}, \quad (7\text{-b})$$

$$\frac{Eh^3}{12\left(1-\nu^2\right)}\left(\frac{\partial^2\varphi_y}{\partial y^2}+\nu\frac{\partial^2\varphi_x}{\partial x\partial y}\right)+\frac{Eh^3}{24\left(1+\nu\right)}\times$$
$$\times\left(\frac{\partial^2\varphi_x}{\partial x^2}+\frac{\partial^2\varphi_y}{\partial x\partial y}\right)-\kappa Gh\left(\varphi_y+\frac{\partial w}{\partial y}\right)=\rho h^3\frac{\partial^2\varphi_y}{\partial t^2}. \quad (7\text{-c})$$

2.4. Higher order shear deformation theory (HSDT)

Another type of plate theory is the third-order shear deformation theory in which the transverse shear stress has a parabolic distribution with respect to the thickness of the plate. Also, there is not any shear correction factor to satisfy the transverse shear stress conditions on the upper and lower layers of the cross-section of the plate. According to Eq. (1), the strain-displacement relations for HSDT can be expressed as:

$$\varepsilon_{xx}=\frac{\partial u_1}{\partial x}=z\frac{\partial\varphi_x}{\partial x}-\frac{4z^3}{3h^2}\left(\frac{\partial\varphi_x}{\partial x}+\frac{\partial^2 w}{\partial x^2}\right), \quad (8\text{-a})$$

$$\varepsilon_{yy}=\frac{\partial u_2}{\partial x}=z\frac{\partial\varphi_y}{\partial y}-\frac{4z^3}{3h^2}\left(\frac{\partial\varphi_y}{\partial y}+\frac{\partial^2 w}{\partial y^2}\right), \quad (8\text{-b})$$

$$\gamma_{xy}=\frac{\partial u_1}{\partial y}+\frac{\partial u_2}{\partial x}=z\left(\frac{\partial\varphi_x}{\partial y}+\frac{\partial\varphi_y}{\partial x}\right)-$$
$$-\frac{4z^3}{3h^2}\left(\frac{\partial\varphi_x}{\partial y}+\frac{\partial\varphi_y}{\partial x}+2\frac{\partial^2 w}{\partial x\partial y}\right), \quad (8\text{-c})$$

$$\gamma_{xz}=\frac{\partial u_1}{\partial z}+\frac{\partial u_3}{\partial x}=\left(1-\frac{4z^2}{h^2}\right)\left(\varphi_x+\frac{\partial w}{\partial x}\right), \quad (8\text{-d})$$

$$\gamma_{yz}=\frac{\partial u_2}{\partial z}+\frac{\partial u_3}{\partial y}=\left(1-\frac{4z^2}{h^2}\right)\left(\varphi_y+\frac{\partial w}{\partial y}\right) \quad (8\text{-e})$$

Using the principle of virtual displacement, the equilibrium equations can be expressed for HSDT as:

$$\frac{\partial Q_{xx}}{\partial x}+\frac{\partial Q_{yy}}{\partial y}-\frac{4}{h^2}\left(\frac{\partial S_{xx}}{\partial x}+\frac{\partial S_{yy}}{\partial y}\right)+$$
$$+\frac{4}{3h^2}\left(\frac{\partial^2 R_{xx}}{\partial x^2}+\frac{\partial^2 R_{yy}}{\partial y^2}+2\frac{\partial^2 R}{\partial x\partial y}\right)=\rho h\frac{\partial^2 w}{\partial t^2}, \quad (9\text{-a})$$

$$\frac{\partial M_{xx}}{\partial x}+\frac{\partial M_{xy}}{\partial y}-\frac{4}{3h^2}\left(\frac{\partial R_{xx}}{\partial x}+\frac{\partial R_{xy}}{\partial y}\right)-Q_{xx}+\frac{4}{h^2}S_{xx}=$$
$$=\rho h^3\frac{\partial^2\varphi_x}{\partial t^2}, \quad (9\text{-b})$$

$$\frac{\partial M_{yy}}{\partial y}+\frac{\partial M_{xy}}{\partial x}-\frac{4}{3h^2}\left(\frac{\partial R_{yy}}{\partial y}+\frac{\partial R_{xy}}{\partial x}\right)-$$
$$-Q_{yy}+\frac{4}{h^2}S_{yy}=\rho h^3\frac{\partial^2\varphi_y}{\partial t^2}, \quad (9\text{-c})$$

where $R=\left\{R_{xx},R_{yy},R_{xy}\right\}^T=\int_{-h/2}^{h/2}z^3\left\{\sigma_{xx},\sigma_{yy},\sigma_{xy}\right\}^T dz$ and

$$S=\left\{S_{xx},S_{yy}\right\}^T=\int_{-h/2}^{h/2}z^2\left\{\sigma_{xz},\sigma_{yz}\right\}^T dz.$$

The governing equations of (9) can be obtained in terms of displacements as:

$$\frac{8Gh}{15}\left(\frac{\partial\varphi_x}{\partial x}+\frac{\partial\varphi_y}{\partial y}+\frac{\partial^2 w}{\partial x^2}+\frac{\partial^2 w}{\partial y^2}\right)+\frac{4Eh^3}{315\left(1-\nu^2\right)}\left[\frac{\partial^3\varphi_x}{\partial x^3}+\right.$$
$$\left.+\frac{\partial^3\varphi_y}{\partial y^3}+\nu\left(\frac{\partial^3\varphi_x}{\partial x\partial y^2}+\frac{\partial^3\varphi_y}{\partial x^2\partial y}\right)\right]-\frac{4Eh^3}{252(1-\nu^2)}\left(\frac{\partial^4 w}{\partial x^4}+\frac{\partial^4 w}{\partial y^4}+\right.$$
$$\left.+2\nu\frac{\partial^4 w}{\partial x^2\partial y^2}\right)+\frac{4Eh^3}{315\left(1+\nu\right)}\left(\frac{\partial^3\varphi_x}{\partial x^2\partial y}+\frac{\partial^3\varphi_y}{\partial x\partial y^2}\right)-$$
$$-\frac{Eh^3}{126\left(1+\nu\right)}\frac{\partial^4 w}{\partial x^2\partial y^2}=\rho h\frac{\partial^2 w}{\partial t^2}, \quad (10\text{-a})$$

$$-\frac{8Gh}{15}\left(\varphi_x+\frac{\partial w}{\partial x}\right)=\rho h^3\frac{\partial^2\varphi_x}{\partial t^2}, \quad (10\text{-b})$$

$$\frac{17Eh^3}{315\left(1-\nu^2\right)}\left(\frac{\partial^2\varphi_y}{\partial y^2}+\nu\frac{\partial^2\varphi_x}{\partial x\partial y}\right)-\frac{4Eh^3}{315\left(1-\nu^2\right)}\times$$
$$\times\left(\frac{\partial^3 w}{\partial y^3}+\nu\frac{\partial^3 w}{\partial x^2\partial y}\right)+\frac{17Eh^3}{630\left(1+\nu\right)}\left(\frac{\partial^2\varphi_x}{\partial x^2}+\frac{\partial^2\varphi_y}{\partial x\partial y}\right)-$$
$$-\frac{4Eh^3}{315\left(1+\nu\right)}\frac{\partial^3 w}{\partial x^2\partial y}-\frac{8Gh}{15}\left(\varphi_y+\frac{\partial w}{\partial y}\right)=$$
$$=\rho h^3\frac{\partial^2\varphi_y}{\partial t^2}. \quad (10\text{-c})$$

3. Nonlocal plate theories for free vibration of SLGSs

3.1. Review of Eringen's nonlocal elasticity

The theory of nonlocal elasticity was first considered by Eringen in the 1970's [25]. This concept is inherent in solid state physics where the nonlocal attractions of atoms are prevalent Eringen. In contrast to the classical elasticity, in the nonlocal model the stress at a reference point x in an elastic body depends not only on the strains at x, but also on strains at all other points of the body [25]. According to the nonlocal elasticity theory, this fact was attributed to the

atomic theory of lattice dynamics and experimental measurements of phonon dispersion [26].

For homogenous and isotropic elastic continuum, the linear nonlocal elasticity theory can be expressed as the following set of equations [26]:

$$\sigma_{kl,k} + \rho\left(f_l - \ddot{u}_l\right) = 0\,, \tag{11-a}$$

$$\sigma_{kl}(x) = \int_V \alpha\left(\left|x - x'\right|, \tau\right)\sigma_{kl}^c(x')dV\,, \tag{11-b}$$

$$\sigma_{kl}^c(x') = L_1 e_{rr}(x')\delta_{kl} + 2L_2 e_{kl}(x')\,, \tag{11-c}$$

$$e_{kl}(x') = \frac{1}{2}\left(\frac{du_k(x')}{dx_l'} + \frac{du_l(x')}{dx_k'}\right). \tag{11-d}$$

Where equation (11-a) is the equilibrium relation in which $\sigma_{kl,l}$, ρ , f_l and u_1 are the nonlocal stress tensor, mass density, body force density and displacement vector at a reference point x in the body, respectively. Eq. (11-b) is the relation between local (σ_{kl}^c) and nonlocal $(\sigma_{kl,l})$ stress tensors using the nonlocal modulus $(\alpha(|x-x'|,\tau))$. Finally, equation (11-c) and (11-d) are the classical constitutive stress-strain and strain-displacement relationships, respectively. L_1 and L_2 are the Lame constants.

Eringen [24] made certain assumptions to simplify equation (11-b) to a partial differential equation form as:

$$(1-\tau^2 l^2\nabla^2)t_{kl}(x) = \sigma_{kl}(x), \tau = e_0\frac{a}{l}\,. \tag{12}$$

Where $t_{kl} = \sigma_{kl,l}$, a/l is the characteristic length ratio and e_0 is the nonlocal constant which are appropriate to the material.

3.2. Application of elastic medium and nonlocal elasticity on beam theories

The nanobeams analyzed in this work are assumed to be embedded in an elastic medium. The elastic surrounding is simulated using Pasternak foundation model [30], which considers both normal pressure and transverse shear stress. So the loading corresponding to this type of foundation model yields as [30]:

$$Q_{Pasternak} = K_w w - K_s\frac{\partial^2 w}{\partial x^2}\,, \tag{13}$$

where K_w is the Winkler modulus parameter corresponding to normal pressure, and K_s is the Pasternak modulus parameter relevant to transverse shear stress.

By neglecting the shear deformation effects $(K_s = 0)$, the foundation model is reduced to Winkler one [29], which represents the normal pressure of elastic medium as a series of closely spaced, vertical linear elastic springs. Thereupon, the loading corresponding to this type of foundation can be expressed as [21].

$$Q_{Winkler} = K_w w\,. \tag{14}$$

In this work, the buckling behavior of nanobeams surrounding in an elastic medium is investigated using both above types of foundation models based on various nonlocal beam theories.

3.2.1. Euler-Bernoulli beam theory

By adding the elastic medium terms to the governing equation of EBT, we will have:

$$-EI\frac{\partial^4 w}{\partial x^4} + K_s\frac{\partial^2 w}{\partial x^2} - K_w w = \rho A\frac{\partial^2 w}{\partial t^2} - \rho I\frac{\partial^4 w}{\partial x^2\partial t^2}\,. \tag{15}$$

Using Eq. (13), the only constitutive relation for nonlocal model of EBT with elastic medium is obtained as:

$$-\left(\mu K_s + EI\right)\frac{\partial^4 w}{\partial x^4} + \left(\mu K_w + K_s\right)\frac{\partial^2 w}{\partial x^2} - K_w w = \\ = \rho A\frac{\partial^2 w}{\partial t^2} - \left(\mu\rho A + \rho I\right)\frac{\partial^4 w}{\partial x^2\partial t^2} + \mu\rho I\frac{\partial^6 w}{\partial x^4\partial t^2}\,. \tag{16}$$

3. 2. 2. Timoshenko beam theory

Adding the elastic medium terms to the governing equations of TBT yields:

$$\left(\kappa GA + K_s\right)\frac{\partial^2 w}{\partial x^2} - K_w w + \kappa GA\frac{\partial\varphi}{\partial x} = \rho A\frac{\partial^2 w}{\partial t^2}\,, \tag{17-a}$$

$$-\kappa GA\frac{\partial w}{\partial x} + EI\frac{\partial^2\varphi}{\partial x^2} - \kappa GA\varphi = \rho I\frac{\partial^2\varphi}{\partial t^2}\,. \tag{17-b}$$

Using equation (13), the constitutive relations for nonlocal model of TBT with elastic medium can be expressed as:

$$-\mu K_s\frac{\partial^4 w}{\partial x^4} + \left(\mu K_w + K_s + \kappa GA\right)\frac{\partial^2 w}{\partial x^2} - K_w w + \\ +\kappa GA\frac{\partial\varphi}{\partial x} = \rho A\frac{\partial^2 w}{\partial t^2} - \mu\rho A\frac{\partial^4 w}{\partial x^2\partial t^2}\,, \tag{18-a}$$

$$-\kappa GA\frac{\partial w}{\partial x} + EI\frac{\partial^2\varphi}{\partial x^2} - \kappa GA\varphi = \rho I\frac{\partial^2\varphi}{\partial t^2} - \\ -\mu\rho I\frac{\partial^4\varphi}{\partial x^2\partial t^2}\,. \tag{18-b}$$

3.2.3. Reddy beam theory

By adding the elastic medium terms to the governing equations of RBT, we will have:

$$-\frac{EI}{21}\frac{\partial^4 w}{\partial x^4} + \left(\frac{8GA}{15} + K_s\right)\frac{\partial^2 w}{\partial x^2} + \frac{16EI}{105}\frac{\partial^3\varphi}{\partial x^3} + \\ +\frac{8GA}{15}\frac{\partial\varphi}{\partial x} - K_w w = \rho A\frac{\partial^2 w}{\partial t^2}\,. \tag{19-a}$$

$$-\frac{16EI}{105}\frac{\partial^3 w}{\partial x^3}-\frac{8GA}{15}\frac{\partial w}{\partial x}+$$
$$+\frac{68EI}{105}\frac{\partial^2 \varphi}{\partial x^2}-\frac{8GA}{15}\varphi=\rho I\frac{\partial^2 \varphi}{\partial t^2}. \quad (19\text{-b})$$

Using equation (13), the constitutive relations for nonlocal model of RBT with elastic medium are obtained as:

$$-\left(\mu K_s+\frac{EI}{21}\right)\frac{\partial^4 w}{\partial x^4}+\left(\mu K_w+K_s+\frac{8GA}{15}\right)\frac{\partial^2 w}{\partial x^2}-$$
$$-K_w w+\frac{16EI}{105}\frac{\partial^3 \varphi}{\partial x^3}+\frac{8GA}{15}\frac{\partial \varphi}{\partial x}=$$
$$=\rho A\frac{\partial^2 w}{\partial t^2}-\mu\rho A\frac{\partial^4 w}{\partial x^2\partial t^2}, \quad (20\text{-a})$$

$$-\frac{16EI}{105}\frac{\partial^3 w}{\partial x^3}-\frac{8GA}{15}\frac{\partial w}{\partial x}+\frac{68EI}{105}\frac{\partial^2 \varphi}{\partial x^2}-\frac{8GA}{15}\varphi=$$
$$=\rho I\frac{\partial^2 \varphi}{\partial t^2}-\mu\rho I\frac{\partial^4 \varphi}{\partial x^2\partial t^2}. \quad (20\text{-b})$$

3. 2. 4. Levinson beam theory

Adding the elastic medium terms to the governing equations of LBT yields:

$$\left(\frac{2GA}{3}+K_s\right)\frac{\partial^2 w}{\partial x^2}-K_w w+\frac{2GA}{3}\frac{\partial \varphi}{\partial x}=\rho A\frac{\partial^2 w}{\partial t^2}, \quad (21\text{-a})$$

$$-\frac{EI}{5}\frac{\partial^3 w}{\partial x^3}-\frac{2GA}{3}\frac{\partial w}{\partial x}+\frac{4EI}{5}\frac{\partial^2 \varphi}{\partial x^2}-\frac{2GA}{3}\varphi=$$
$$=\rho I\frac{\partial^2 \varphi}{\partial t^2}. \quad (21\text{-b})$$

Using Eq. (13), the constitutive relations for nonlocal model of LBT with elastic medium can be expressed as:

$$-\mu K_s\frac{\partial^4 w}{\partial x^4}+\left(\mu K_w+K_s+\frac{2GA}{3}\right)\frac{\partial^2 w}{\partial x^2}-$$
$$-K_w w+\frac{2GA}{3}\frac{\partial \varphi}{\partial x}=$$
$$=\rho A\frac{\partial^2 w}{\partial t^2}-\mu\rho A\frac{\partial^4 w}{\partial x^2\partial t^2}, \quad (22\text{-a})$$

$$-\frac{EI}{5}\frac{\partial^3 w}{\partial x^3}-\frac{2GA}{3}\frac{\partial w}{\partial x}+\frac{4EI}{5}\frac{\partial^2 \varphi}{\partial x^2}-\frac{2GA}{3}\varphi=$$
$$=\rho I\frac{\partial^2 \varphi}{\partial t^2}-\mu\rho I\frac{\partial^4 w}{\partial x^2\partial t^2}. \quad (22\text{-b})$$

It is worth to mention that by removing the surrounded elastic medium effects from the governing equations corresponding to each beam theory, they reduce to the conventional nonlocal beam theories presented by Reddy [27].

4. Analytical solution for simply supported nanobeams

4.1. Explicit formulas for natural frequencies

In this section, exact solutions of free vibration of nanobeams embedded in an elastic medium are developed. Explicit formulas are proposed to obtain the natural frequencies corresponding to each nonlocal beam theory. The simply supported boundary conditions can be expressed as:

$$w(0)=w(L)=0, \quad (23\text{-a})$$

$$M(0)=M(L)=0. \quad (23\text{-b})$$

The components of displacement w and φ can be considered in the following generalized form which satisfies the boundary conditions:

$$w(x,t)=\sum_{m=1}^{\infty}W_m sin\left(\frac{m\pi x}{L}\right)e^{i\omega_m t}, \quad (24\text{-a})$$

$$\varphi(x,t)=\sum_{m=1}^{\infty}\phi_m cos\left(\frac{m\pi x}{L}\right)e^{i\omega_m t}. \quad (24\text{-b})$$

Substituting Eqs. (25) in the constitutive relations of different nonlocal beam theories and solving the resulting eigenvalue problem, the natural frequencies of nanobeams embedded in an elastic medium can be obtained.

For Euler-Bernoulli beam theory, the natural frequencies can be expressed as:

$$\omega_{EBT}^2=\frac{\left(m^4\pi^4\mu K_s+m^4\pi^4 EI+m^2\pi^2\mu K_w L^2+\right.}{\left(m^2\pi^2\rho A\mu L^2+\rho AL^4\right)}$$
$$\frac{\left.+m^2\pi^2 K_s L^2+K_w L^4\right)}{\left(m^2\pi^2\rho A\mu L^2+\rho AL^4\right)}. \quad (25)$$

For Timoshenko beam theory, the natural frequencies can be obtained as follows:

$$\omega_{TBT}^2=(m^6\pi^6\mu K_s EI+m^4\pi^4\mu K_s\kappa GAL^2+$$
$$+m^4\pi^4\mu K_w EIL^2+m^2\pi^2\mu K_w\kappa GAL^4+$$
$$+m^4\pi^4 K_s EIL^2+m^2\pi^2 K_s\kappa GAL^4+$$
$$+m^4\pi^4\kappa GAEIL^2+m^2\pi^2 K_w EIL^4+$$
$$+K_w\kappa GAL^6). \quad (26)$$

For Reddy beam theory, the natural frequencies can be expressed as:

$$\omega_{RBT}^2=\frac{1}{5}(85m^6\pi^6\mu K_s EI+70m^4\pi^4\mu K_s GAL^2+$$
$$+m^6\pi^6 E^2 I^2+70m^4\pi^4 EIGAL^2+85m^4\pi^4\mu K_w EIL^2+$$
$$+70m^2\pi^2\mu K_w GAL^4+85m^4\pi^4 K_s EIL^2+$$
$$\frac{+70m^2\pi^2 K_s GAL^4+85m^2\pi^2 K_w EIL^4+}{+(17m^2\pi^2\rho AEIL^4+14\rho GA^2L^6+}$$
$$\frac{+70K_w GAL^6)}{+17m^4\pi^4\mu\rho AEIL^2+14m^2\pi^2\mu\rho GA^2L^4)}. \quad (27)$$

For Levinson beam theory, the natural frequencies can be obtained as follows:

$$\omega_{LBT}^2 = (6m^6\pi^6\mu K_s EI + 5m^4\pi^4\mu K_s GAL^2 + \\ +6m^4\pi^4\mu K_w EIL^2 + 5m^2\pi^2\mu K_w GAL^4 + \\ +6m^4\pi^4 K_s EIL^2 + 5m^2\pi^2 K_s GAL^4 + \\ +5m^4\pi^4 GAEIL^2 + 6m^2\pi^2 K_w EIL^4 + \\ +5K_w GAL^6)/(6m^2\pi^2\rho AEIL^4 + 5\rho GA^2L^6 + \\ +6m^4\pi^4\rho A\mu EIL^2 + 5m^2\pi^2\rho GA^2L^4). \quad (28)$$

4.2. Numerical results and discussion

Here the numerical results are presented for the developed analytical solution in the previous section. The following properties are taken for the nanobeams which are used by Reddy [27].

$$E = 30\times10^6\ \mathrm{N/m^2},\ \nu = 0.3,\ \rho = 1.$$

It is assumed that h=b=1 nm and L varies from $\frac{L}{h} = 10$ to 50.

The non-dimensional natural frequencies corresponding to the first three modes of the nanotubes are given in Tables 1-3. It's found from the results that with increasing the value of nonlocal parameter the values of natural frequencies decrease, especially for lower aspect ratios. It implies that the nonlocality effect is more significant for the shorter nanobeams and this effect tends to decrease the stiffness of the nanobeam. Moreover, the small-size effect is more prominent at higher mode numbers.

Table 1

Non-dimensional natural frequencies $\left(\omega\times L^2\sqrt{\frac{\rho A}{EI}}\right)$ of the first mode

L/h	μ	*EBT* $K_w=0$ $K_s=0$	*EBT* $K_w=20$ $K_s=2$	*TBT* $K_w=0$ $K_s=0$	*TBT* $K_w=20$ $K_s=2$	*RBT* $K_w=0$ $K_s=0$	*RBT* $K_w=20$ $K_s=2$	*LBT* $K_w=0$ $K_s=0$	*LBT* $K_w=20$ $K_s=2$
10	0	9.8696	9.8737	9.7519	9.7561	9.7520	9.7561	9.7713	9.7756
	0.5	9.6347	9.6389	9.5199	9.5241	9.5199	9.5241	9.5387	9.5432
	1	9.4159	9.4202	9.3036	9.3080	9.3036	9.3080	9.3220	9.3266
	1.5	9.2113	9.2157	9.1015	9.1059	9.1015	9.1059	9.1195	9.1241
	2	9.0195	9.0240	8.9119	8.9165	8.9120	8.9165	8.9296	8.9343
20	0	9.8696	9.9344	9.8398	9.9048	9.8398	9.9048	9.8400	9.9050
	0.5	9.8093	9.8745	9.7796	9.8450	9.7796	9.8450	9.7798	9.8452
	1	9.7501	9.8156	9.7206	9.7864	9.7206	9.7864	9.7208	9.7866
	1.5	9.6919	9.7579	9.6626	9.7288	9.6626	9.7288	9.6628	9.7291
	2	9.6347	9.7011	9.6056	9.6722	9.6056	9.6722	9.6059	9.6725
50	0	9.8696	12.1420	9.8648	12.1381	9.8648	12.1381	9.8648	12.1381
	0.5	9.8599	12.1341	9.8551	12.1302	9.8551	12.1302	9.8552	12.1303
	1	9.8502	12.1262	9.8454	12.1224	9.8454	12.1224	9.8454	12.1225
	1.5	9.8405	12.1184	9.8357	12.1145	9.8357	12.1145	9.8357	12.1146
	2	9.8309	12.1106	9.8261	12.1067	9.8261	12.1067	9.8261	12.1068

Table 2

Non-dimensional natural frequencies $\left(\omega\times L^2\sqrt{\frac{\rho A}{EI}}\right)$ of the second mode

L/h	μ	*EBT* $K_w=0$ $K_s=0$	*EBT* $K_w=20$ $K_s=2$	*TBT* $K_w=0$ $K_s=0$	*TBT* $K_w=20$ $K_s=2$	*RBT* $K_w=0$ $K_s=0$	*RBT* $K_w=20$ $K_s=2$	*LBT* $K_w=0$ $K_s=0$	*LBT* $K_w=20$ $K_s=2$
10	0	39.4784	39.4795	37.6906	37.6917	37.6925	37.6936	37.7615	37.7626
	0.5	36.0779	36.0791	34.4441	34.4453	34.4459	34.4471	34.5152	34.5164
	1	33.4277	33.4289	31.9139	31.9152	31.9155	31.9168	31.9848	31.9861
	1.5	31.2870	31.2883	29.8702	29.8716	29.8717	29.8731	28.9410	29.9424
	2	29.5111	29.5125	28.1747	28.1762	28.1761	28.1776	28.2454	28.2469
20	0	39.4784	39.4948	39.0077	39.0243	39.0079	39.0244	39.0088	39.0253
	0.5	38.5390	38.5557	38.0795	38.0964	38.0796	38.0966	38.0805	38.0975
	1	37.6635	37.6807	37.2145	37.2318	37.2146	37.2320	37.2155	37.2329
	1.5	36.8452	36.8627	36.4059	36.4236	36.4060	36.4237	36.4069	36.4246
	2	36.0779	36.0958	35.6478	35.6659	35.6479	35.6660	35.6489	35.6669
50	0	39.4784	40.1077	39.4020	40.0324	39.4020	40.0324	39.4021	40.0325
	0.5	39.3235	39.9552	39.2473	39.8802	39.2473	39.8802	39.2475	39.8804
	1	39.1704	39.8045	39.0945	39.7298	39.0945	39.7298	39.0947	39.7300
	1.5	39.0190	39.6555	38.9434	39.5812	38.9434	39.5812	38.9435	39.5814
	2	38.8694	39.5083	38.7941	39.4343	38.7941	39.4343	38.7943	39.4346

Table 3

Non-dimensional natural frequencies $\left(\omega \times L^2 \sqrt{\frac{\rho A}{EI}}\right)$ of the third mode

L/h	μ	*EBT* $K_w = 0$ $K_s = 0$	*EBT* $K_w = 20$ $K_s = 2$	*TBT* $K_w = 0$ $K_s = 0$	*TBT* $K_w = 20$ $K_s = 2$	*RBT* $K_w = 0$ $K_s = 0$	*RBT* $K_w = 20$ $K_s = 2$	*LBT* $K_w = 0$ $K_s = 0$	*LBT* $K_w = 20$ $K_s = 2$
10	0	88.8264	88.8269	80.4687	80.4693	80.4875	80.4880	80.6519	80.7705
	0.5	73.9161	73.9166	66.9613	66.9619	66.9769	66.9775	67.1418	67.0963
	1	64.6414	64.6421	58.5593	58.5600	58.5729	58.5737	58.6917	58.8105
	1.5	58.1622	58.1630	52.6897	52.6906	52.7020	52.7028	52.8208	52.8216
	2	53.3078	53.3087	48.2921	48.2930	48.3033	48.3042	48.4221	48.4230
20	0	88.8264	88.8338	86.4953	86.5029	86.4968	86.5043	86.5000	86.5075
	0.5	84.2711	84.2789	82.0595	82.0675	82.0609	82.0689	82.0643	82.0723
	1	80.3517	80.3598	78.2429	78.2513	78.2443	78.2526	78.2477	78.2560
	1.5	76.9327	76.9412	74.9137	74.9224	74.9150	74.9237	74.9185	74.9271
	2	73.9161	73.9249	71.9762	71.9853	71.9774	71.9865	71.9808	71.9899
	Table 3 continued								
50	0	88.8264	89.1084	88.4408	88.7240	88.4408	88.7240	88.4411	88.7243
	0.5	88.0478	88.3323	87.6655	87.9512	87.6655	87.9513	87.6659	87.9517
	1	87.2893	87.5762	86.9103	87.1985	86.9103	87.1985	86.9107	87.1989
	1.5	86.5500	86.8394	86.1742	86.4649	86.1742	86.4649	86.1746	86.4653
	2	85.8292	86.1210	85.4566	85.7496	85.4566	85.7497	85.4569	85.7501

Also, it can be seen that by considering the influence of transverse shear strain using *TBT*, *RBT*, and *LBT*, the values of natural frequencies will be reduced for all values of nonlocal parameter specifically for higher modes. Furthermore, the difference between *TBT* and *RBT* is so negligible for the first mode, but it is relatively more sensible for higher modes and lower aspect ratios.

By incorporating the elastic foundation, the non-dimensional natural frequencies increase for all values of nonlocal parameter which indicates that surrounding in an elastic medium makes the nanobeams stiffer and at the first mode, this increase of stiffness is more prominent for higher values of aspect ratio. However, for higher modes, the effect of elastic medium tends to be independent from the value of aspect ratio. Fig. 1 depicts this pattern in more sensible way, in which the slope of variation of non-dimensional natural frequency with the value of aspect ratio decreases for higher mode numbers.

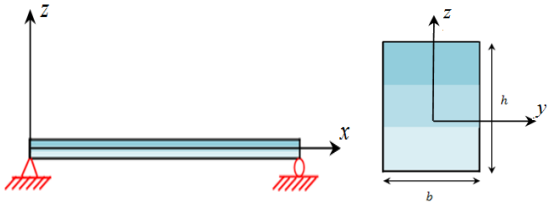

Fig. 1 Simply supported straight uniform plate with rectangular cross section and its coordinate system

It should be noted that the results depicted in Fig. 2 and the other Figures are corresponding to Reddy beam theory, and because there is not any consequential difference between the behaviors of various beam theories, the results of other beam theories are not given for brevity. The Winkler modulus parameter effect on the value of natural frequency of nanobeams with different aspect ratios is plotted in Fig. 3. It is assumed that $\mu = 1$ and the nanobeam is represented as Winkler foundation model $(K_s = 0)$. The Winkler modulus parameter is taken in the range of 0-400 used by Liew et al. [31]. This range of K_w includes the interval of soft elastic medium to a very stiff one. It can be observed that the effect of K_w is more considerable for higher values of aspect ratio.

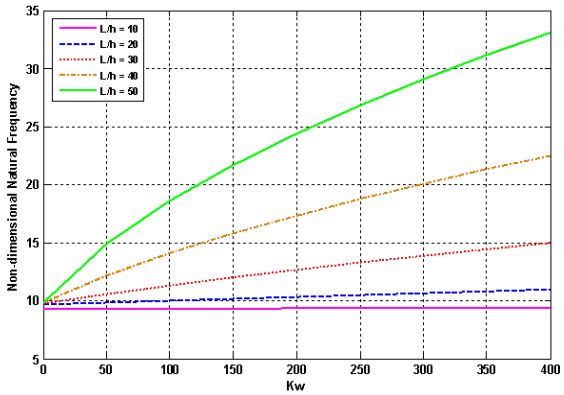

Fig. 2 Variation of non-dimensional natural frequency with Winkler modulus parameter corresponding to different values of aspect ratio $(\mu = 1)$

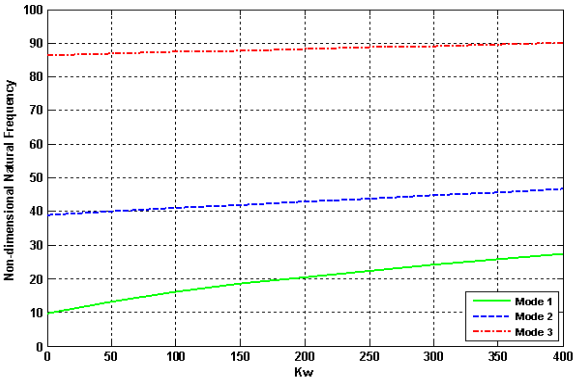

Fig. 3 Variation of non-dimensional natural frequency with Winkler modulus parameter corresponding to different mode numbers $(\mu = 1,\ L/h = 45)$

To investigate the effect of Pasternak modulus parameter on the vibrational behavior of nanobeams, the variation of non-dimensional natural frequency of nanobeam with the value of Pasternak modulus parameter is depicted in Fig. 4 corresponding to different nonlocal parameters. The surrounding elastic medium is simulated as Pasternak foundation model with $K_w = 100$. Fig. 4-a shows this effect for $L/h = 10$ and Fig. 4-b shows this effect corresponding to $L/h = 50$. It can be found that as the aspect ratio of nanobeams increases K_s has more significant influence on the value of critical buckling load.

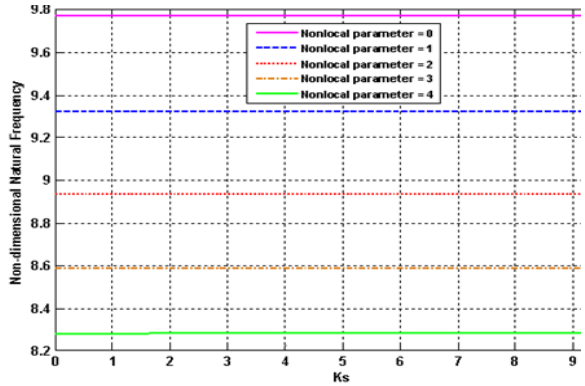

a

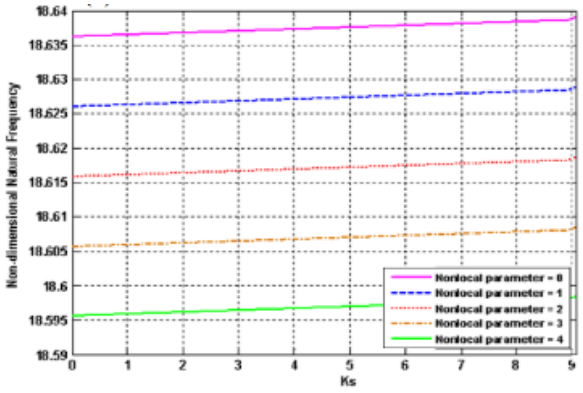

b

Fig. 4 Effect of Pasternak modulus parameter on non-dimensional natural frequency for different values of nonlocal parameter: (a) $K_w = 100$, $L/h = 10$, (b) $K_w = 100$, $L/h = 50$

The mode-shapes for the transverse displacement w and angular displacement φ corresponding to various Winkler modulus parameter and nonlocal parameter are shown in Fig. 5. In all cases, the configuration of mode-shapes are obtained at $w_{max} = 1.0$. There is not any significant difference between mode-shapes for various aspect ratios, so they are described just corresponding to $L/h = 10$ for brevity. It can be observed that the mode-shapes relevant to simply supported-simply supported boundary conditions have not any sensible dependency to the both values of Winkler modulus parameter and nonlocal parameter.

Fig. 6 indicates the difference between the natural frequencies obtained by Winkler foundation model and the Pasternak one. To this end, the variation of non-dimensional natural frequencies with the value of aspect ratio is plotted corresponding to both foundation models. It is assumed that $\mu = 1$ throughout the range of aspect ratio and $K_w = 20$, $K_s = 0$ for Winkler foundation model and $K_w = 20$, $K_s = 2$ for Pasternak foundation model.

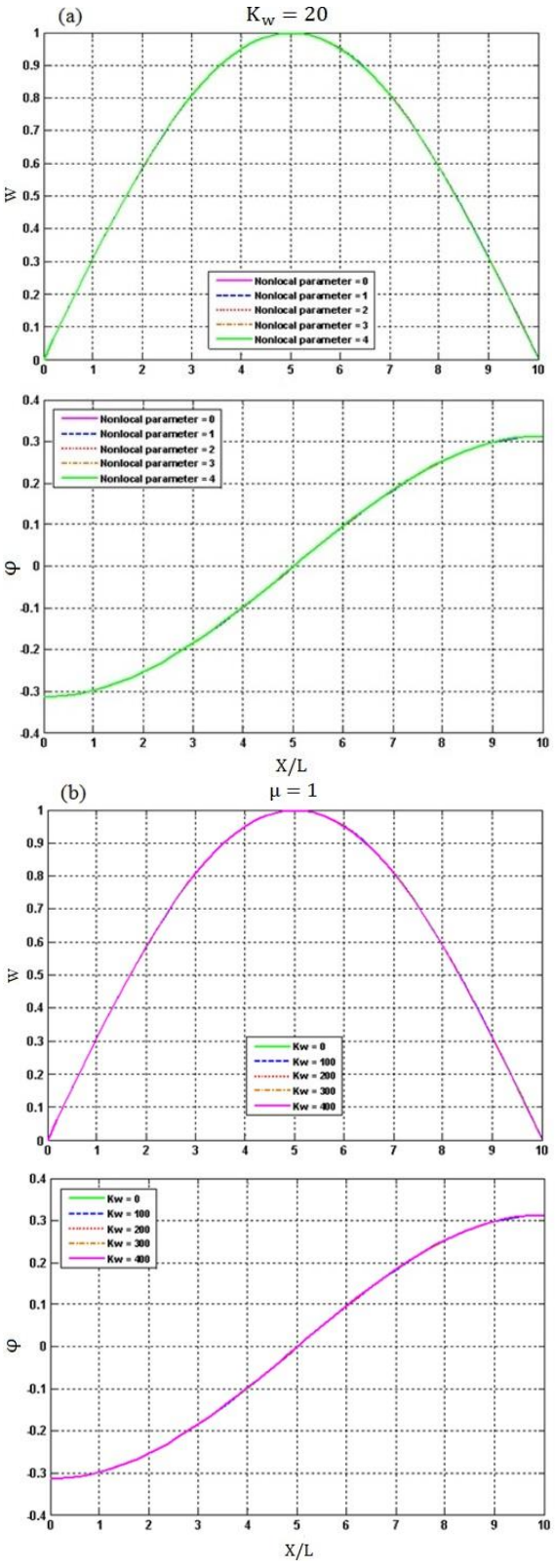

Fig. 5 Effects of nonlocal parameter and Winkler modulus parameter on the mode-shapes of transverse and angular displacements with: (a) K_w=20; (b) μ=1

As shown in the Fig. 6, for each aspect ratio, the calculated natural frequency with the Winkler-based models

is lower than the natural frequency calculated by the Pasternak models. More, as the value of aspect ratio increases the difference between two foundation models increases too. This reveals that alike the observation from Fig. 4, Pasternak modulus parameter has more significant influence at higher values of aspect ratio.

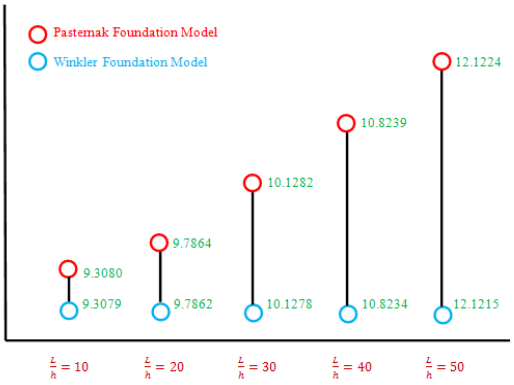

Fig. 6 Comparison of non-dimensional natural frequency obtained with Winkler and Pasternak foundation models corresponding to different values of aspect ratio

5. Conclusion

In the present study, free vibrational response of embedded SLGSs is investigated. To this end, Eringen's nonlocal elasticity continuum is incorporated into the various plate theories namely as classical plate theory (CLPT), first order shear deformation theory (FSDT), and higher order shear deformation theory (HSDT) to consider the size-effects on the vibration analysis of SLGSs. Both Winkler and Pasternak elastic foundation models are employed to represent the surrounding elastic medium. Explicit expressions are derived through an analytical solution to evaluate the natural frequencies corresponding to each type of nonlocal plate model.

Selected numerical results are presented to indicate the influence of the values of nonlocal parameter, Winkler modulus parameter, Pasternak modulus parameter, mode number, aspect ratio, and the type of nonlocal plate theory, in detail. It is observed that in contrast to the implementation of nonlocality which causes to reduce the stiffness of SLGS, by taking into account of elastic foundation, the natural frequency increases for all values of nonlocal parameter and this effect is more significant for higher aspect ratios relevant to all mode numbers which is again in contrast to the nonlocality effect that is more considerable in the lower aspect ratios. Also, it is found that the fundamental frequency of embedded SLGSs simulated by Pasternak foundation model is relatively more than the ones simulated by Winkler foundation model and this difference is approximately similar for all types of nonlocal plate theories. Moreover, it is observed that the difference between the two types of elastic foundation model is more prominent for higher values of nonlocal parameter and aspect ratio.

References

1. **Lian, P.; Zhu, X.; Liang, S.; Li, Z.; Yang**, **W.; Wang, H.** 2010. Large Reversible Capacity of High Quality Graphene Sheets as an Anode Material for Lithium-Ion Batteries, Electro chimica Acta 55(12): 3909-3914, http://dx.doi.org/10.1016/j.electacta.2010.02.025.
2. **Wu, Z.P.; Wang**, **J.N.** 2009. Preparation of Large-Area Double-Walled Carbon Nanotube Films and Application as Film Heater, Physica E 42(1): 77-81, http://dx.doi.org/10.1016/j.physe.2009.09.003.
3. **Kitipornchai, S.; He, X. Q.; Liew**, **K.M.** 2005. Continuum Model for the Vibration of Multilayered Graphene Sheets, Physical Review B 72(7): 075443. http://dx.doi.org/10.1103/PhysRevB.72.075443.
4. **Liew, K.M.; He, X.Q.; Kitipornchai**, **S.** 2006. Predicting Nanovibration of Multi-Layered Graphene Sheets Embedded in an Elastic Matrix, ActaMaterialia 54(16): 4229-4236. http://dx.doi.org/10.1016/j.actamat.2006.05.016.
5. **Azizi, S.; Safaei, B.; Fattahi, A. M.; Tekere, M.** 2015. Nonlinear Vibrational Analysis of Nanobeams Embedded in an Elastic Medium including Surface Stress Effects, Advanced in Materils Since and Engineering: 1-7. http://dx.doi.org/10.1155/2015/318539.
6. **Azizi, S.; Fattahi, A. M.; Kahnamouei, J. T.** 2015. Evaluating mechanical properties of nanoplatelet reinforced composites under mechanical and thermal loads, Computational and Theoretical Nanoscience 12: 4179-4185.
7. **Shen, L.; Shen, H.S.; Zhang**, **C. L.** 2010. Nonlocal Plate Model for Nonlinear Vibration of Single Layer Graphene Sheets in Thermal Environment, Computational Materials Science 48(3): 680-685. http://dx.doi.org/10.1016/j.commatsci.2010.03.006.
8. **Pradhan, S.C.; Phadikar**, **J.K.** 2009. Small Scale Effect on Vibration of Embedded Multilayered Graphene Sheets based on Nonlocal Continuum Models, Physics Letters A 373 (11): 1062-1069. http://dx.doi.org/10.1016/j.physleta.2009.01.030.
9. **Narendar, S.; Gopalakrishnan**, **S.** 2009. Nonlocal Scale Effects on Wave Propagation in Multi-Walled Carbon Nanotubes, Computational Materials Science 47(2): 526-538. http://dx.doi.org/10.1016/j.commatsci.2009.09.021.
10. **Murmu, T.; Pradhan**, **S.C.** 2009. Thermo-Mechanical Vibration of a Single-Walled Carbon Nanotube Embedded in an Elastic Medium based on Nonlocal Elasticity Theory, Computational Materials Science 46(4): 854-859. http://dx.doi.org/10.1016/j.comatsci.2009.04.019.
11. **Sahmani, S.; Fattahi**, **A.M.** 2017. An anisotropic calibrated nonlocal plate model for biaxial instability analysis of 3D metallic carbon nanosheets using molecular dynamics simulations, 4 (6): .1-14, http://dx.doi.org/10.1088/2053-1591/aa6bc0.
12. **Fattahi, A. M.; Sahmani, S.** 2017. Nonlocal temperature-dependent postbuckling behavior of FG-CNT reinforced nanoshells under hydrostatic pressure combined with heat conduction, Microsystem Technologies, Microsystem Technologies 23 (10): 5121–5137. http://dx.doi.org/10.1007/s00542-017-3377-x.
13. **Fattahi, A.M.; Najipour**, **A.** Experimental study on mechanical properties of PE / CNT composites, Journal of Theoretical and Applied Mechanics 55(2): 719-726, http://dx.doi.org/10.15632/jtam-pl.55.2.719.
14. **Sahmani, S.; Fattahi**, **A.M.** 2016. Size-dependent nonlinear instability of shear deformable cylindrical nano-

panels subjected to axial compression in thermal environments, Microsystem Technologies 23(10): 4717–4731.
http://dx.doi.org/10.1007/s00542-016-3220-9.
15. **Fattahi, A.M.; Safaei**, **B.** 2017. Buckling analysis of CNT-reinforced beams with arbitrary boundary conditions, Microsystem Technologies 23(10): 5079–5091. http://dx.doi.org/10.1007/s00542-017-3345-5.
16. **Sahmani, S.; Fattahi**, **A.M.** 2017. Calibration of developed nonlocal anisotropic shear deformable plate model for uniaxial instability of 3D metallic carbon nanosheets using MD simulations, Computer Methods in Applied Mechanics and Engineering, 322: 187-207. http://dx.doi.org/10.1016/j.cma.2017.04.015.
17. **Sahmani, S.; Fattahi**, **A.M.** 2017. Development an efficient calibrated nonlocal plate model for nonlinear axial instability of zirconia nanosheets using molecular dynamics simulation, J. Mol. Graph. Model 75: 20–31. http://dx.doi.org/10.1016/j.jmgm.2017.04.018.
18. **Kaveh E. Torkanpouri; Hassan Zohoor; Moharam H. Korayem.** 2017. Global sensitivity analysis of backside coating parameters on dynamic response of AM-AFM, MECHANIKA 22(3):282-290. http://dx.doi.org/10.5755/j01.mech.23.2.13908.
19. **Ali Yousefzadi Nobakht; Seungha Shin; Kenneth D Kihm; Drew C Marable; Woomin Lee.** 2017. Heat flow diversion in supported graphene nanomesh, Carbon 123: 45-53. http://dx.doi.org/10.1016/j.carbon.2017.07.025.
20. **Rasool Moradi-Dastjerdi; Hamed Momeni-Khabisi**. 2017. Vibrational behavior of sandwich plates with functionally graded wavy carbon nanotube-reinforced face sheets resting on Pasternak elastic foundation, Journal of Vibration and Control. http://dx.doi.org/10.1177/1077546316686227.
21. **Winkler**, **E.** 1867. in: Theory of Elasticity and Strength, Dominicus, Prague.
22. **Pasternak**, **P.L.** 1954. On a New Method of Analysis of an Elastic Foundation by means of Two Foundation Constants, Gos, Izd, Lip, po Strait I Arkh.
23. **Pradhan, S.C.; Murmu**, **T.** 2010. Small Scale Effect on the Buckling Analysis of Single-Layered Graphene Sheet Embedded in an Elastic Medium based on Nonlocal Plate Theory, Physica E 42(5): 1293-1301. http://dx.doi.org/10.1016/j.physe.2009.10.053.
24. **Liew, K.M.; He, X.Q.; Kitipornchai**, **S.** 2006. Predicting Nanovibration of Multi-Layered Graphene Sheets Embedded in an Elastic Matrix, Acta Materialia 54(16): 4229-4236. http://dx.doi.org/10.1016/j.actamat.2006.05.016.
25. **Eringen**, **A.C.** 1972. Linear Theory of Nonlocal Elasticity and Dispersion of Plane Waves, International Journal of Engineering Science 10(5): 425-435. http://dx.doi.org/10.1016/0020-7225(72)90050-X.
26. **Eringen**, **A.C.** 1983. On Differential Equations of Nonlocal Elasticity and Solutions of Screw Dislocation and Surface Waves, Journal of Applied Physics 54(9): 4703-4710. http://dx.doi.org/10.1063/1.332803.
27. **Reddy, J.N.** 2007. Nonlocal theories for bending, buckling and vibration of beams, International Journal of Engineering Science V45:288-307. http://dx.doi.org/10.1016/j.ijengsci.2007.04.004.

Babak Safaei, A.M. Fattahi

FREE VIBRATIONAL RESPONSE OF SINGLE-LAYERED GRAPHENE SHEETS EM-BEDDED IN AN ELASTIC MATRIX USING DIFFERENT NONLOCAL PLATE MODELS

S u m m a r y

In this paper, the small scale effects are incorporated into the free vibration analysis of single-layered graphene sheets (SLGSs) embedded in an elastic medium. To this end, Eringen's nonlocal elasticity continuum are applied to the different types of plate theory namely as the classical plate theory (CLPT), first order shear deformation theory (FSDT), and higher order shear deformation theory (HSDT). Winkler and Pasternak foundation models used to simulate the surrounding elastic medium are compared with each other. Explicit expressions are derived to calculate the natural frequencies of square SLGSs corresponding to each type of nonlocal plate model. Selected numerical results are given to indicate the influence of the nonlocal parameter, Winkler and Pasternak elastic moduli, mode number, and the side length of SLGSs in detail. Also, comparison is made between the vibrational responses of SLGSs obtained through different nonlocal plate theories. It is found that the elastic foundation and value of nonlocal parameter have quite significant effects on the natural frequencies of SLGSs and these effects are influenced by mode number as well as side length.

Keywords: graphene sheets; free vibrations; nonlocal elasticity; exact solution; elastic foundation.

Received April 30, 2016
Accepted October 13, 2017